Algorithms of chaotic data sequences processing

Roman Voliansky[1,*,†], Nina Volianska[1,†] and Arief Bramanto Wicaksono Putra[2,†]

[1] National Technical University of Ukraine "Igor Sikorsky Kyiv Polytechnic Institute", Polytechnichna Str., 37, Kyiv, 03056, Ukraine

[2] Politeknik Negeri Samarinda, Str. Jl. Cipto Mangun Kusumo, Samarinda, 75242, Indonesia

Abstract

Our paper is devoted to the design of methodological backgrounds to extend the class of chaotically generated data. Our backgrounds are based on the coordinate transformation of the system phase portrait, which is given in the orthogonal coordinates into non-orthogonal coordinate systems. We consider both coordinate systems in the plane and in some space. We provide the transformations from the initial coordinate system to the target one as discrete-time expressions. From the control theory viewpoint, one can consider these expressions as observability equations, whose discrete-time nature allows one to consider them as the basis for implementing some data processing routines. These routines take the signals from chaotic and/or regular generators as input information. We offer to produce this information by using the master-slave principle and considering the generator as some driven device. We think such an approach allows performing the synchronization of several generators from one source if it is necessary to use many intermediate signals to produce output one. We consider both cases of master device which use information about the generator state or do not use any. As an example of our approach's usage to process the chaotic data, we consider transforming the Duffing pendulum-based chaotic oscillator's output to various coordinate systems.

Keywords

chaotic system, coordinate transformation, non-orthogonal coordinates, observability equation

1. Introduction

Nowadays, data transmission using chaotic systems [1, 2, 3] refers to the practical usage of chaos theory [4, 5, 6] and chaotic signals [7, 8] to secure information transmission. Chaotic systems are susceptible to initial conditions and exhibit complex, unpredictable behavior over time [9, 10, 11]. These facts about chaotic systems make them useful in secure communication [12, 13] because chaotic signals can be difficult to predict, intercept, or reproduce without knowing the exact system parameters [14, 15, 16].

Such unique chaotic systems' features cause several key concepts in chaotic communication:

- Chaotic modulation involves embedding information into a chaotic signal [17, 18, 19]. The chaotic signal acts as a carrier wave, which is then modulated by the data. Only receivers knowledgeable about the chaotic system's parameters can demodulate and recover the original message.
- Synchronization of chaotic systems requires the transmitter and receiver must use identical or synchronized chaotic systems [20, 21, 22]. These systems must be synchronized so the receiver can extract the embedded message from the chaotic signal.
- Chaotic masking assumes the data signal is added to a chaotic carrier signal at the transmitter end [23, 24, 25]. The chaotic signal masks the data, making it indistinguishable from noise to

ADP'24: International Workshop on Algorithms of Data Processing, November 5, 2024, Kyiv, Ukraine

* Corresponding author.

† These authors contributed equally.

voliansky@ua.fm (R. Voliansky); ninanin@i.ua (N. Volianska); ariefbram@gmail.com (A.B.W. Putra)

0000-0001-5674-7646 (R. Voliansky); 0000-0001-5996-2341 (N. Volianska); 0000-0003-1187-5040 (A.B.W. Putra)

an eavesdropper. The receiver, knowing the chaotic system, can subtract the chaotic carrier and retrieve the original data.

- The noise-like signals concept assumes that chaotic signals appear similar to noise, making them hard to distinguish from random background noise in the communication channel [26, 27, 28]. This property provides inherent security, as an eavesdropper without the system parameters will find it challenging to extract meaningful data.

The above-shown concepts find their practical implementation in designing various chaotic modulation schemes. The main ones are Chaos Shift Keying (CSK) [29, 30] and Chaotic Phase Modulation (CPM) [31, 32]. These modulation schemes find their applications in establishing wireless communications. In this case, chaotic communication can be applied in wireless systems where robustness to interference is crucial. Since chaotic signals are noise-like and spread across a wide bandwidth, they can be used in environments with high electromagnetic interference. Also, various optical fiber communication systems use laser signals to transmit data securely [33, 34]. Optical chaos can be generated using semiconductor lasers, and synchronization between transmitter and receiver can be achieved with optical feedback.

In summary, chaotic systems offer a promising approach to secure data transmission by leveraging the unpredictable and noise-like nature of chaos, making it difficult for unauthorized parties to intercept or decode the communication

We offer to avoid this drawback by using coordinate transformations to give the considered system the desired features and put it attractor in the desired M-dimensional domain of coordinate system. Our method is demonstrating by considering a 2nd order chaotic system which is based on the Duffing pendulum usage.

The paper is organized as follows: firstly, we show some general transformations of the driven chaotic system into discrete-time domain. Then we show the design of observability equations to define system motions in the generalized non-orthogonal coordinates in plane and space We illustrate the use of our approach by studying a well-known Duffing equation transformation. Finally, we make a conclusion.

2. Methods and materials

2.1. The generalized oscillator's equation

Let us consider the simplest conservative 2nd order dynamical system:

$$\ddot{x} = -\omega^2 x, \tag{1}$$

where x is a system output and ω is some factor.

It is a well-known fact that with non-zero initial conditions:

$$\dot{x}(0) = dx_0; \quad x(0) = x_0 \tag{2}$$

solution of (1) can be found in following class of harmonic functions:

$$x(t) = \frac{dx_0}{\omega}\sin(\omega t) + x_0\cos(\omega). \tag{3}$$

So, one can consider implementation of (3) as a generator of regular harmonic oscillations with frequency ω, which amplitude depends on system initial conditions.

Since the use of trigonometric functions can cause some implementation problems by using digital devices due to a quite long time to define values of these functions, one can use (1) instead of (3) to design a harmonic generator. In this case, equation (1) should be transformed into discrete-time domain by using known approximations of derivative operator. We consider it in the most general case as follows:

$$\ddot{x}(t) = \frac{d^2x}{dt^2}x \approx f_2(x, z^{-1}x, z^{-2}x, T), \tag{4}$$

where T is a sample time, z^{-i} is a shift operator which usage means taking the i-th previously defined value of variable x. Index 2 near function f means approximation of 2nd order derivative.

Substitution of (4) into (1) allows us to write down 2nd order finite difference equation for the considered generator:

$$x = g_2(z^{-1}x, z^{-2}x, T, \omega), \tag{5}$$

where $g_2(.)$ is a solution of (1) and (4) for x.

Expression (5) allows us to define an element of regular data series by using known previous values and cyclic iteration of (5) allows us to get whole data series. One can use this series in various applications which need harmonic signal generator.

At the same time some applications require more complex form of oscillations. That is why we turn our attention in (1) and generalize it by using some external non-monotonic signal $u(t)$ which is processed with nonlinear function $h_{xu}(u)$ as well as replacing linear feedback term with nonlinear sign-variable finite function $h_{xx}(x)$:

$$\ddot{x} = -h_{xx}(x) + h_{xu}(u(t)). \tag{6}$$

We call (6) as the generalized externally driven oscillator's equation in the continuous-time domain. It is clear that motion trajectory of (6) is uniquely determined by functions $h_{xx}(.)$ and $h_{xu}(.)$ which allow producing both regular and chaotic oscillations.

Since nowadays most of signals produced by digital devices, we rewrite it into discrete-time domain by substituting (4) into (6) and solving it for x:

$$x = g_2(h_{xx}(z^{-1}x), h_{xx}(z^{-2}x), h_{xu}(u((i-1)T)), T), i \in [0, \infty), \tag{7}$$

where i is a current sample number.

Analysis of (7) shows highly nonlinearity of its right-and expression. Moreover, it shows the necessity to define nonlinear feedback signals for two previous time moment. Because function $h(.)$ can be defined by quite complex expression, its calculation for various signals can require a lot of time and other calculation resources. That is why we offer to simplify (7) by taking into account that in the previous time moment signal $z^{-2}x$ is considered as $z^{-1}x$ and memorized for future use:

$$x = g_2(h_{xx}(z^{-1}x), z^{-1}M, h_{xu}(u((i-1)T)), T), M = h_{xx}(z^{-1}x), i \in [0, \infty). \tag{8}$$

One can use (8) to implement the generalized generator, which is able to produce nonlinear data sequences. The main feature of this generator is its time-dependence while signal u is defined. So, the internal clock signal should be used to implement (8). We call (8) as the generalized nonlinear generator's equation which differ from known ones by the possibility of multiply usage some previous memorized signals or their combinations as well as an open range of samples number.

The last fact can cause some problems in real implementation of the considered discrete-time dynamical system in digital devices with limited hardware resources due to the necessity to operate with big numbers after some operating time. We offer to avoid this problem by considering dynamic of subsystem which produces signal $u(iT)$ jointly with subsystem which produces system output x. We call the first subsystem as excitator and the second one as generator. In the most general case, these systems are interconnected as it is shown in Figure 1.

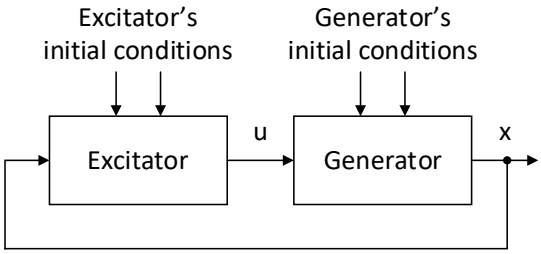

Figure 1: Block-diagram of closed-loop excitatory-generator system.

One can use the expressions which are similar to (8) and define dynamic of subsystems in Figure 1 as follows:

$$\begin{aligned} x &= g_{2x}(h_{xx}(z^{-1}x), z^{-1}M_x, h_{xu}(z^{-1}u), T), \quad M_x = h_x(z^{-1}x), \\ u &= g_{2u}(h_{uu}(z^{-1}u), z^{-1}M_u, h_{ux}(z^{-1}x), T), \quad M_u = h_u(z^{-1}u), \end{aligned} \tag{9}$$

where g_{2x}, g_{2u}, h_{xx}, h_{uu}, h_{xu}, h_{ux} are some functions which defines motions of the considered system, M_x and M_u are memorized peace of information for generator and excitor subsystems.

It is clear that system (9) does not use any information about current system time so it can be used to produce high frequency signals without the necessity to use any system clock or timers with very small sample time.

We call (9) as equations of the generalized nonlinear oscillator with integrated nonlinear excitatory and iterations of these equations defines the algorithms to process chaotic data x by using the generated sequence u. In the most general case, all subsystems interrelate each other and make closed loop dynamical system. All subsystems are considered as driven one and each of them drive another one. In the particular case one can consider the open-loop system by removing feedback from generator output to excitatory input. In this case only generator should be considered as a driven subsystem and excitator is an autonomous device which produce some oscillations according to its inner algorithm. System equations in this case can be simplified as follows:

$$\begin{aligned} x &= g_{2x}(h_{xx}(z^{-1}x), z^{-1}M_x, h_{xu}(z^{-1}u), T), \qquad & M_x &= h_x(z^{-1}x), \\ u &= g_{2u}(h_{uu}(z^{-1}u), z^{-1}M_u, T), & M_u &= h_u(z^{-1}u). \end{aligned} \tag{10}$$

Both of (9) and (10) allows to implement digital devices which produce some oscillations. The form and other parameters of these oscillations depend on the functions which are used in the right-hand expressions of these formulas. One can make these oscillations more complex if extend the terms M_j and consider them as some vectors which are used to store proceeded data from several previous system states. One can use known control methods to analyze the stability of system motions and prove that undamped oscillations occur in the designed in such a way discrete-time system.

2.2. Observability equations based on non-orthogonal coordinate system use

The use of nonlinear functions g_{2x}, g_{2u}, h_{xx}, h_{uu}, h_{xu}, h_{ux} while generator's dynamic is being defined allows to form oscillations which are complex enough. At the same time, it is quite hard to form the desired system dynamic by using only (9) because of closed-loop system usage.

That is why we offer to follow the known from control theory approach which is based on the use of state space equations. In the most general case such an equation can be defined as the nonlinear combination of generator and exciter state variables:

$$y = g_y(x, z^{-1}x, z^{-1}M_x, u, z^{-1}u, z^{-1}M_u), \tag{11}$$

where $g_y(.)$ is some nonlinear function.

One can append (11) to system (9) to define the state space equations for the considered driven generator. Moreover, he can use several observability equations with different $g_y(.)$ functions to design a multichannel generator and form several signals at the same time. Numerical calculations according to (11) and (9) makes strong backgrounds for chaotic signal generating and processing.

It is clear that no any limitations on class and parameters of function $g_y(.)$ and one can use any single or multivariable functions to define the generator output variables. Due to a very wide class of the functions which can be potentially used a lot of methods of their determination exist. In our paper we offer to use an approach which is based on coordinate transformations from orthogonal *N*-dimensional coordinate system into *M*-dimensional non-orthogonal ones.

One can perform such transformations by considering dynamical system motion in the 2D cartesian plane and in some *N*-dimensional space. Let us consider the above-mentioned transformations in detail.

2.3. Observability equation in M-dimensional non-orthogonal coordinates' plane

Let us consider an orthogonal state plane which orths are defined by using x and u state variables from (10). We define in this plane some non-orthogonal coordinate system which origin is shifted from the origin of xu plane in x_0 and u_0, this non-orthogonal coordinate system has three axes y_1,

y_2 and y_3 the angles between y_1 and y_2 is α_1 and between y_2 and y_3 is α_2. The angle between y_1 axis and axis x equals to β (Figure 2). We think that each from y_i axes has its own scale factors s_i.

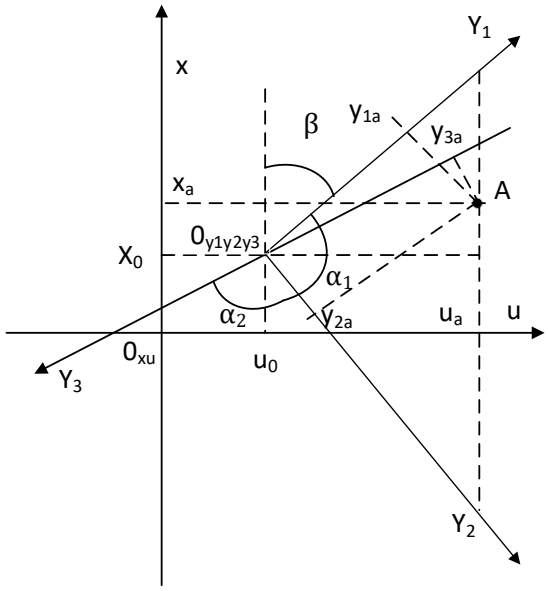

Figure 2: Positions of system's representative point A in different coordinates.

The simple trigonometric transformations give us the possibility to write down following expressions that define interrelations between point positions in different coordinate bases:

$$\begin{gathered} y_{1a} = (x_a - x_0)\cos(\beta) + (u_a - u_0)\sin(\beta); \\ y_{2a} = (x_a - x_0)\cos(\beta + \alpha_1) + (u_a - u_0)\sin(\beta + \alpha_1); \\ y_{3a} = (x_a - x_0)\cos(\beta + \alpha_1 + \alpha_2) + (u_a - u_0)\sin(\beta + \alpha_1 + \alpha_2). \end{gathered} \quad (12)$$

Analysis of (12) allows us to generalize the component of point A position in some axis y_i:

$$y_{ia} = (x_a - x_0)\cos\left(\beta + \sum_{j=1}^{i}\alpha_j\right) + (u_a - u_0)\sin\left(\beta + \sum_{j=1}^{i}\alpha_j\right). \quad (13)$$

Observability equations (12) and (13) are defined for the case the same scales in axes. If one take into account the different scales in the axes, (13) can be rewritten as follows:

$$y_{ia} = s_{ix}(x_a - x_0)\cos\left(\beta + \sum_{j=1}^{i}\alpha_j\right) + s_{iu}(u_a - u_0)\sin\left(\beta + \sum_{j=1}^{i}\alpha_j\right), \quad (14)$$

where s_{ix} and s_{iu} are scale factors for signals in x and u axes.

Expression (14) define interrelation between system position in the orthogonal and non-orthogonal coordinates. This equation is linear for x_a and u_a if other factors are constants.

It is necessary to say that one can use as many axes in non-orthogonal coordinates as he likes and the studied system in non-orthogonal coordinates can be considered as linear or nonlinear dependent one. This expression can be considered as the solution of direct problem of system position transformation into new coordinate system. Analysis of the above-obtained expression shows that new coordinate system can be at least first order one. In this case the system position is defined as point in the axis y_1. In other words, observability equations' usage allows us to decrease and increase of system output's order.

Because the initial system position is defined in the state plane it is necessary to define at least two observability equations to solve the inverse problem of determination system state variable x and u by its output signals y_1 and y_2:

$$u_a = \frac{u_0 sin(\alpha_1) - y_1\cos(\beta + \alpha_1) + y_2 cos(\beta)}{\sin(\alpha_1)}; \quad (15)$$

$$x_a = \frac{x_0 sin(\alpha_1) - y_1 \sin(\beta + \alpha_1) - y_2 sin(\beta)}{\sin(\alpha_1)}.$$

The use of (15) allows us to define system state variables by its known outputs and can be considered as some intermediate step in identifying the reasons that caused the observed system motions.

In the considered case we study defining of observability equations when system state variables are interpreted as coordinates of some orthogonal state plane. But this case cannot be considered as the only one. Thus, one can assume that system state variable x defines system linear position and u defines its angular position in polar coordinate system. In this case (14) should be rewritten in such a way:

$$y_{ia} = s_{ix}(x_a \sin(u_a) - x_0)\cos\left(\beta + \sum_{j=1}^{i} \alpha_j\right) + \mathrm{s}_{iu}(x_a \cos(u_a) - u_0)\sin\left(\beta + \sum_{j=1}^{i} \alpha_j\right). \quad (16)$$

Due to the nonlinearity of (16) its solution for x_a and u_a can be performed only in the numerical way. So, the defining of system state variables in this case can be quite untrivial problem by using conventional digital devices due to the necessity to perform a big amount of calculations to solve nonlinear equations in the real time mode.

Generally speaking, one can consider any term from (14) as system state variable but not only position of A point. We think that one can assume the constant values of point A coordinate and consider components of origin $O_{y_1 y_2 y_3}$ position x_0 and u_0 as system state variables. Another way to interpret system (9) outputs is their consideration as scale factors s_{ix} and s_{iu}. It is clear that all above-considered cases allow operating with weights near trigonometric functions which values are considered as constants. The more complex observability equation can be defined if one takes two angles from the angles' set and consider them as inputs for the observability equation. In this case (14) can be rewritten in such a way:

$$y_{ia} = C_1 \cos\left(\beta + \mathrm{x} + \mathrm{u} + \sum_{j=3}^{i} \alpha_j\right) + C_2 \sin\left(\beta + \mathrm{x} + \mathrm{u} + \sum_{j=3}^{i} \alpha_j\right), \quad (17)$$

$$C_1 = s_{ix}(x_a - x_0); C_2 = \mathrm{s}_{iu}(\mathrm{u}_a - u_0).$$

Contrary to the observability equation (14) which has variable factors near constants trigonometric functions values, expression (17) is defined with variable arguments of trigonometric functions which are weighted with some constants C_i.

The all above-given cases are considered for two variables which are produced by generator and excitator in Figure 1. This fact limits the number of variables that are used in the (14) and (16). At the same time, it is possible to increase the number of variables in the designed observability equations if one takes into account previous system states. Various linear and nonlinear combinations of state variables of (9) make it possible to define all terms in (14) as variable ones which depend on the studied system state. Such an approach allows considering motions of the generator and axes where these motions are defined. Under term axes motion we understand the changing of each component of their origin position in a separate way with its own linear speed. We assume that in the most general case, the rotation of each axis is happening with its own angular speed and each axis can change its scale.

Thus, one can consider the calculations according to the above-given observability equations as performing complex data post-process routine to improve the designed system features. One can apply this routine in the different ways. From the one hand, it can be used for immediate processing of the generated data. For example, one can find this approach is useful to process non-regular data. From another hand, the regular data can be generated and its one period can be saved in some memory storage. We call such data as core data. Then various observability equations with different parameters and/or algorithms of their changings can be applied to the data to make system output more complex. It is clear that the second way to produce system output can be considered as using of some freezed core data using. Moreover, contrary to the conventional approach in signal

generating when data is produced continuously, one can turn of the generator after core data is obtained and saved to reduce the consumption of calculation resources or allocate their use for another purposes.

2.4. Nonlinear observability equation in M-dimensional non-orthogonal state space

One more complex way to improve system performance is the use of observability equation which is defined not in plane but in some space. In Figure 3 we show the above considered orthogonal 2D plane (red lines) in which coordinates of representative point A are defined. This plane is taken into 3D orthogonal (blue lines) and non-orthogonal (black lines) spaces.

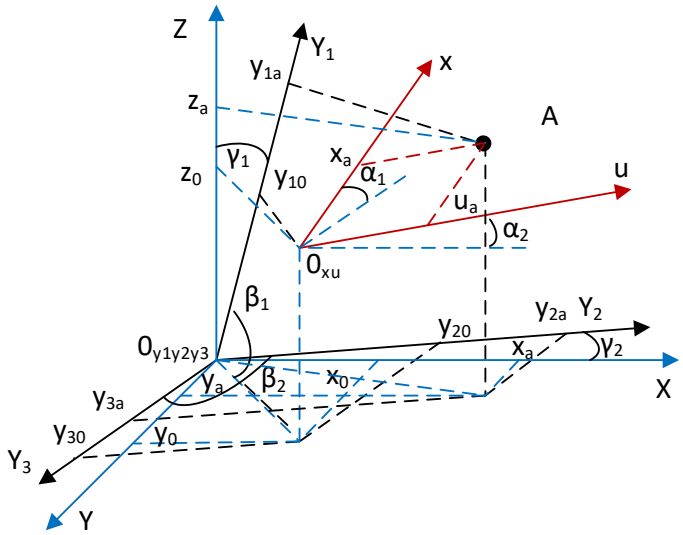

Figure 3: Representative point position in 3D state spaces.

At first, we offer to define position of representative point in the extended orthogonal coordinates:

$$x_a = x_0 + u_a\cos(\alpha_2);\ y_a = y_0 - x_a\cos(\alpha_1);\ \ z_a = z_0 + x_a\sin(\alpha_1) + u_a\sin(\alpha_2). \quad (18)$$

Expressions (18) allows us to define the position of the representative point, which is given in 2D plane, in 3D space by taking into account the plane origin's position and orientation. The use of such an approach gives the possibility to increase the number of output variables similar to previous considered approach but using other interrelations between state space coordinates and system outputs. Since the signs in (18) depend on axes directions one can generalize it by using following expressions for *M* dimensional state space:

$$x_{ia} = x_{i0} + u_{ia}\cos(\alpha_i);\ \ z_i = z_0 + \sum_{i=1}^{m} u_{ia}\sin(\alpha_i), \quad (19)$$

where u_{ia} is a position of representative point in i-th axis, α_i is an angle between i-th axis and plane.

One can make one more generalization of (19) by taking into account scale factors s_i:

$$x_{ia} = s_i(x_{i0} + u_{ia}\cos(\alpha_i));\ \ z_i = s_i\left(z_0 + \sum_{i=1}^{m} u_{ia}\sin(\alpha_i)\right). \quad (20)$$

Expressions (20) gives us the possibility to define m-th sized system outputs by using the system state variables as well as factors of shift, scale and rotate of coordinate axes. These outputs are defined as some projections of system representative point' position in some M-dimensional space. Due to the algebraic form of these expressions one can use them to define system position under stationary and variable transformation factors.

Moreover, one can use (20) as the initial orthogonal coordinates to define system position in the non-orthogonal coordinates. We offer to use the approach which we consider in the previous subsection and define system position in non-orthogonal coordinates as follows:

$$y_{ia} = (x_{ia} - x_{i0})\cos\left(\gamma_i + \sum_{j=1}^{i}\beta_j\right) + (\mathrm{x}_{ia} - x_{io})\sin\left(\gamma_2 + \sum_{j=1}^{i}\beta_j\right), i = 1..m, \quad (21)$$

where we assume that variables x_i means coordinates in non-orthogonal base.

Thus, in the most general case the produced by generator data should be transformed into M-dimensional orthogonal space according to (20) and then expression (21) should be applied to obtain system output in the non-orthogonal coordinates. It is clear that both transformations (20) and (21) can be applied to the (9) with assumption that all transformation factors have variable values which are defined as system state variables or their combinations as well as combinations of their previous values. We believe that this fact allows to define the huge range of system output signals.

3. Results and discussions

3.1. Duffing pendulum model with the nonlinear excitator

Let us consider the well-known second order Duffing equation into normal form (6):

$$\ddot{x} = -b_1\dot{x} - b_2x - b_3x^3 + b_4\cos(b_5t), \quad (22)$$

where x is a pendulum position, b_i are pendulum factors, t is system time.

Signal in the last summand of (22) can be obtained as the result of solution the following second order ordinary differential equation (ODE):

$$\ddot{u} = -b_5^2u, \;\; u(0) = 1, \qquad \dot{u}(0) = 0. \quad (23)$$

Thus, the Duffing pendulum model in continuous time can be given in such a way:

$$\begin{aligned} &\ddot{x} = -b_1\dot{x} - b_2x - b_3x^3 + b_4u, \;\; x(0) = 0, \qquad \dot{x}(0) = 0; \\ &\ddot{u} = -b_5^2u, \qquad\qquad\qquad\quad u(0) = 1, \qquad \dot{u}(0) = 0. \end{aligned} \quad (24)$$

To represent (24) into discrete time domain, at first, we rewrite it as the system of fourth first order ODE:

$$\begin{aligned} &\dot{x}_1 = x_2; \quad \dot{x}_2 = -b_1x_2 - b_2x_1 - b_3x_1^3 + b_4u_1, \;\; x_1(0) = 0, \qquad x_2(0) = 0; \\ &\dot{u}_1 = u_2; \quad \dot{u}_2 = -b_5^2u_1, \qquad\qquad\qquad\qquad\quad u_1(0) = 1, \qquad u_2(0) = 0, \end{aligned} \quad (25)$$

and then apply first order feedback difference approximation of derivative operator:

$$\frac{d}{dt} \approx \frac{1 - z^{-1}}{z^{-1}T} \quad (26)$$

to each equation of (25):

$$\begin{aligned} x_1 &= z^{-1}x_1 + z^{-1}Tx_2, \qquad x_1(0) = 0; \\ x_2 &= (1 - Tb_1)z^{-1}x_2 - Tb_2z^{-1}x_1 - Tb_3z^{-1}x_1^3 + Tb_4z^{-1}u_1, \qquad x_2(0) = 0; \\ u_1 &= z^{-1}u_1 + z^{-1}Tu_2, \qquad u_1(0) = 1; \\ u_2 &= z^{-1}u_2 - Tb_5^2z^{-1}u_1, \;\; u_2(0) = 0. \end{aligned} \quad (27)$$

We call (27) as discrete-time model of Duffing pendulum with cosine-like excitator.

Results of numerical solution of (27) are given in Figure 4. We consider following factors of (27) in our simulations: $T = 10^{-4}$ s, $b_1 = 0.02$, $b_2 = 1$, $b_3 = 5$, $b_4 = 8$, $b_5 = 0.5$. Equations (27) are implemented as some code for Arduino Due board, which performs all calculations, obtained results transmitted to PC with simple serial communication.

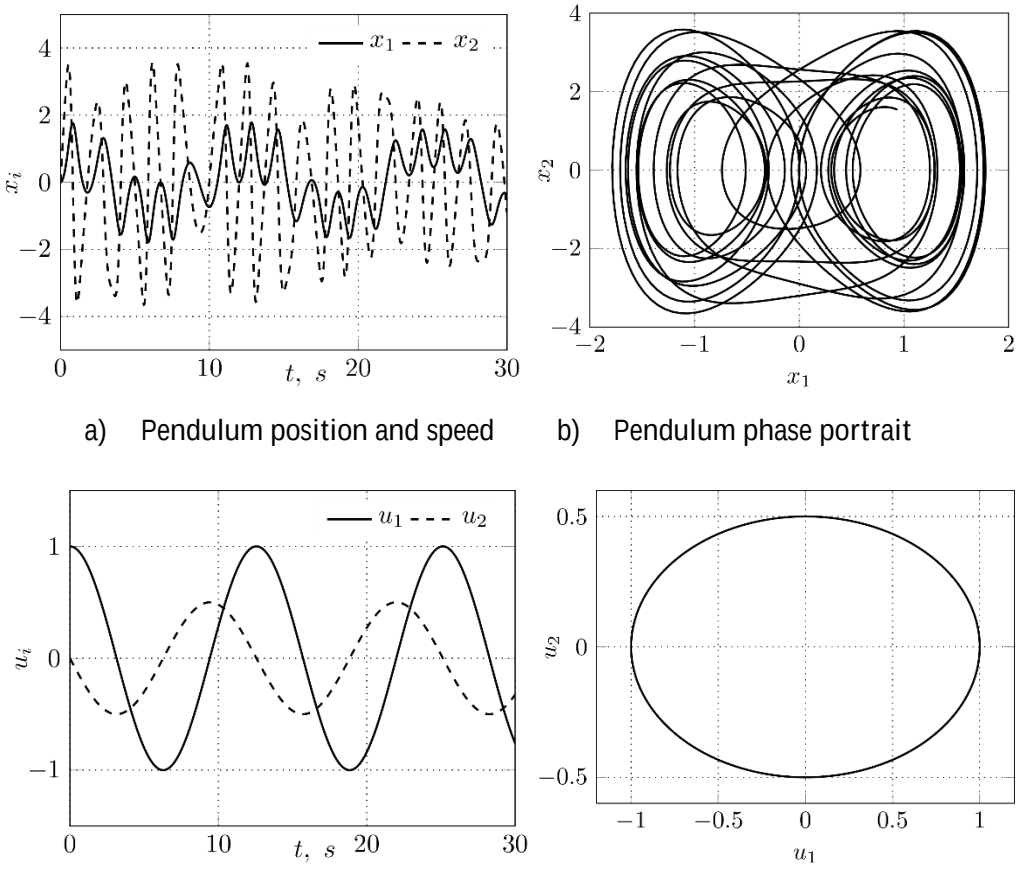

a) Pendulum position and speed b) Pendulum phase portrait

c) Excitator position and speed d) Excitator phase portrait

Figure 4: Duffing pendulum simulation results.

Comparison of the above-given curves with known ones shows they are the same. This fact proves the correctness of our transformation from the continuous time to the discrete time domain.

One can make the Duffing excitatory nonlinear by applying some nonlinear function to its last summand. We believe that such changing gives us the possibility to get new pendulum motion trajectories and give it new features. Unfortunately, study of such system is out of our paper scope, so we leave it for future research. Here we only define the class of possible nonlinear functions as class of variable-sign nonlinear functions. Such class selection we explain the necessity to get not monotonic risen coordinate u which can cause occurring big signals and lead calculation overflows.

In our study we use one of function from the above-mentioned class:

$$f(u,v)=\begin{cases} abs(u)^v & if \quad u>0, \\ 0 & if \quad u=0, \\ -abs(u)^v & if \quad u<0, \end{cases} \tag{28}$$

where $abs(.)$ means taking absolute value from the u signal.

Substitution of this function into (27) allows us to rewrite it as follows

$$\begin{aligned} x_1 &= z^{-1}x_1 + z^{-1}Tx_2, \qquad x_1(0)=0; \\ x_2 &= (1-Tb_1)z^{-1}x_2 - Tb_2z^{-1}x_1 - Tb_3z^{-1}x_1^3 + Tb_4z^{-1}u_1, \qquad y_2(0)=0; \\ u_1 &= z^{-1}u_1 + z^{-1}Tu_2, \qquad u_1(0)=1; \\ u_2 &= z^{-1}u_2 - Tb_5^2 f(z^{-1}u_1, v), \quad u_2(0)=0. \end{aligned} \tag{29}$$

Simulation results for various parameter v are shown in Figure 5.

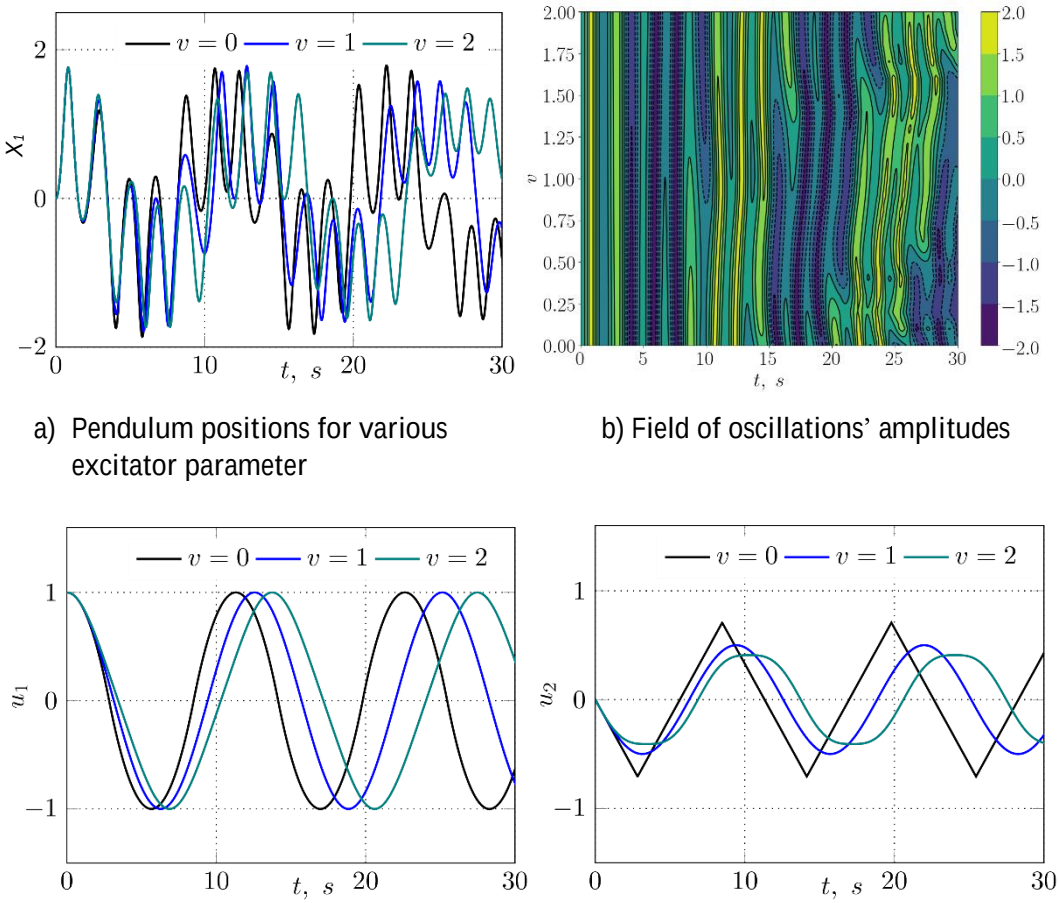

a) Pendulum positions for various excitator parameter

b) Field of oscillations' amplitudes

c) Excitator output u_1

d) First derivative of excitator output

Figure 5: Duffing pendulum with nonlinear excitatory.

Analysis of the solution of (29) proves the possibility to change Duffing pendulum dynamic by changing form of excitatory oscillations. As one can see, the use of nonlinear functions in the excitatory equation change form of its output oscillations and effects on Dufding pendulum motions by shifting peaks of its oscillations in right when power factor in nonlinear function is increased.

Equations (29) define pendulum motion without using of feedback signal about pendulum position. One can claim that these equations are the example of (10). But taking into account information about variable y_1 while u_2 is being defined allows us to design an excitator which is driven by pendulum position:

$$\begin{aligned} x_1 &= z^{-1}x_1 + z^{-1}Tx_2, & y_1(0) &= 0; \\ x_2 &= (1 - Tb_1)z^{-1}x_2 - Tb_2z^{-1}x_1 - Tb_3z^{-1}x_1^3 + Tb_4z^{-1}u_1, & y_2(0) &= 0; \\ u_1 &= z^{-1}u_1 + z^{-1}Tu_2, & u_1(0) &= 1; \\ u_2 &= z^{-1}u_2 - Tb_5^2 f(z^{-1}u_1, v) - Tb_6z^{-1}x_1, & u_2(0) &= 0. \end{aligned} \tag{30}$$

Oscillations which are produced by (30) are shown in Figure 6.

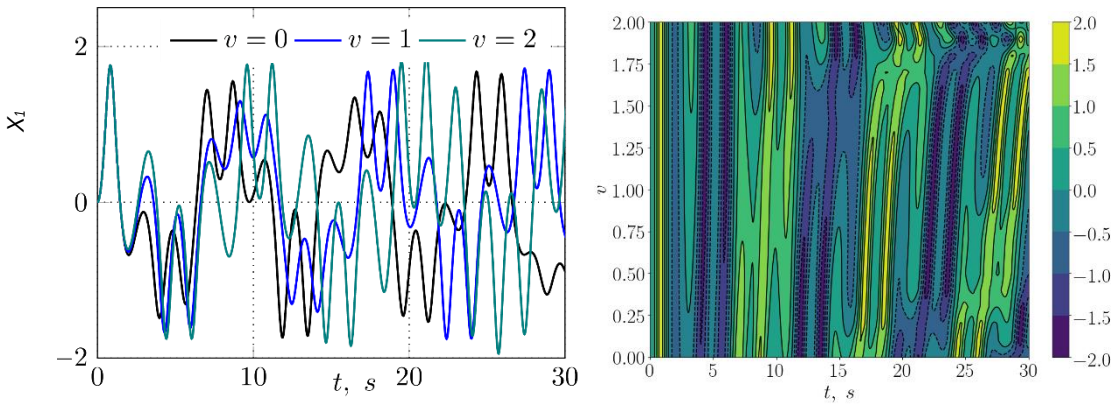

a) Pendulum positions for various excitator parameter

b) Field of oscillations' amplitudes

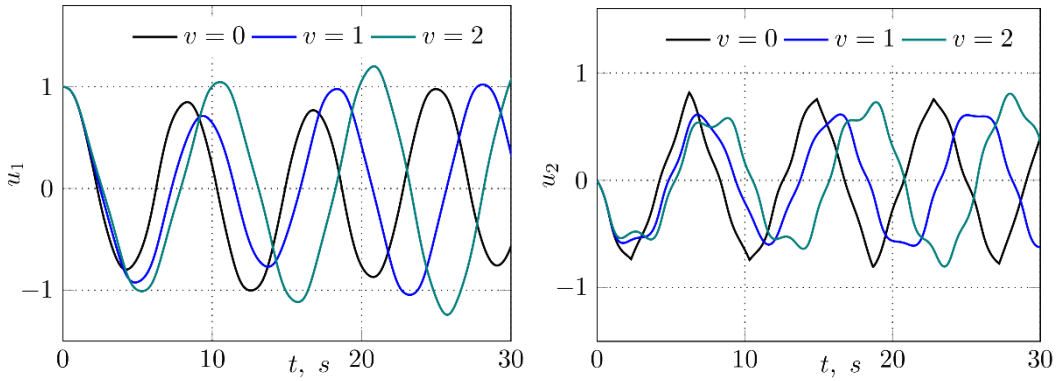

c) Excitator output u_1

d) First derivative of excitator output

Figure 6: Duffing pendulum with chaotic driven nonlinear excitatory with $b_6 = 0.2$.

As one can see the use of driven oscillator allows us to make pendulum motion more unpredictable and form more complex oscillations. This fact is proven by analysis of fields in Figure 5b and Figure 6b which shows that in the system with driven excitatory chaos becomes earlier and only one first oscillation can be considered as regular one.

3.2. Duffing pendulum model in M-dimensional non-orthogonal coordinates' plane

The above designed models (29) and (30) illustrate the effect of driven regular or chaotic oscillations on pendulum motions. If one implements these models, he can design novel chaotic generator with new features. At the same time, analysis of the curves in Figure 5, Figure 6 and comparison them with Figure 4 shows the same common patterns in oscillations forming.

That is why we offer to append (30) with (14). In our paper we study the case of dynamical system with three outputs. Since the considered generator's dynamic is defined by four state variables, one can write down different observability equations.

We offer to use the following equations for the case when all parameters of observability equation are considered as independent variables:

$$\begin{gathered} x_1 = s_{ix}(y_1 - x_0)\cos(\beta) + s_{iu}(u_1 - u_0)\sin(\beta); \\ x_2 = s_{ix}(y_1 - x_0)\cos(\beta + \alpha_1) + s_{iu}(u_1 - u_0)\sin(\beta + \alpha_1); \\ x_3 = s_{ix}(y_1 - x_0)\cos(\beta + \alpha_1 + \alpha_2) + s_{iu}(u_1 - u_0)\sin(\beta + \alpha_1 + \alpha_2). \end{gathered} \quad (31)$$

Simulation results for the system (30) with observability equations (31) are given in Figure 7 for the case of constant factors equals to one.

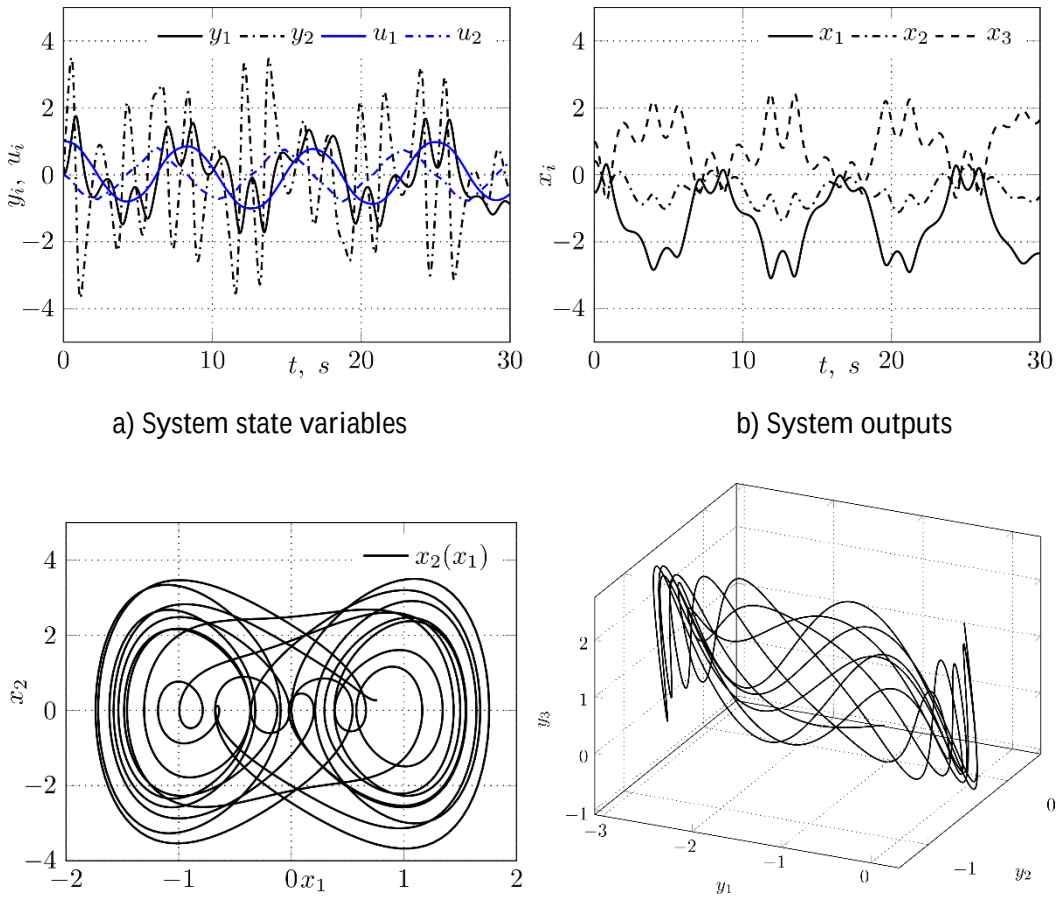

a) System state variables

b) System outputs

c) System 2D phase portrait

d) System 3D attractor

Figure 7: Simulation results of pendulum with observability equations (31).

Here and further, we take into account the three-channel system output and consider system motions in some virtual orthogonal 3D state space to show signals interrelations. At the same time, the designed system is still considered in some plane where it has phase portrait which is shown in Figure 7c. This phase portrait is same for all systems which are considered in current subsection. Figure 8 shows simulation results for case of harmonically changed factors which usage means the determination of pendulum position in rotating coordinates. Here we assume that angles $\beta, \alpha_1, \text{and } \alpha_2$ are defined by sine functions with angular speeds 1, 2, and 3 rad/s. Also, we think that origin position x_0 and u_0 are defined by cosine function with angular speeds 5 and 10 rad/s and scale factors are changed with speeds 1 and 2.

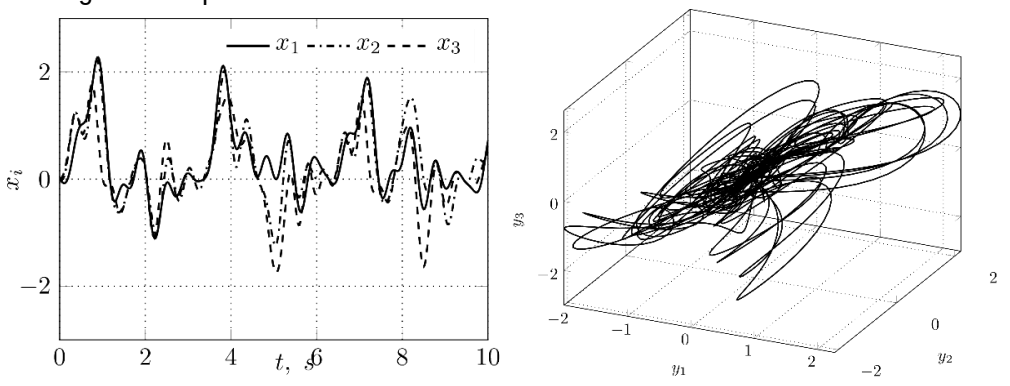

a) System outputs

b) System 3D attractor

Figure 8: Simulation results of pendulum with observability equations (31) with variable factors.

As one can see regular motions of system factors make output motions highly chaotic.

In Figure 9 we show simulation for the case when origin position is defined by using internal state variables of (14):

$$\begin{gathered} x_1 = s_{ix}(y_1 - u_2)\cos(\beta) + s_{iu}(u_1 - y_2)\sin(\beta); \\ x_2 = s_{ix}(y_1 - u_2)\cos(\beta + \alpha_1) + s_{iu}(u_1 - y_2)\sin(\beta + \alpha_1); \\ x_3 = s_{ix}(y_1 - u_2)\cos(\beta + \alpha_1 + \alpha_2) + s_{iu}(u_1 - y_2)\sin(\beta + \alpha_1 + \alpha_2). \end{gathered} \quad (32)$$

This figure is given for the case of constant angles between axes as well as scale factors.

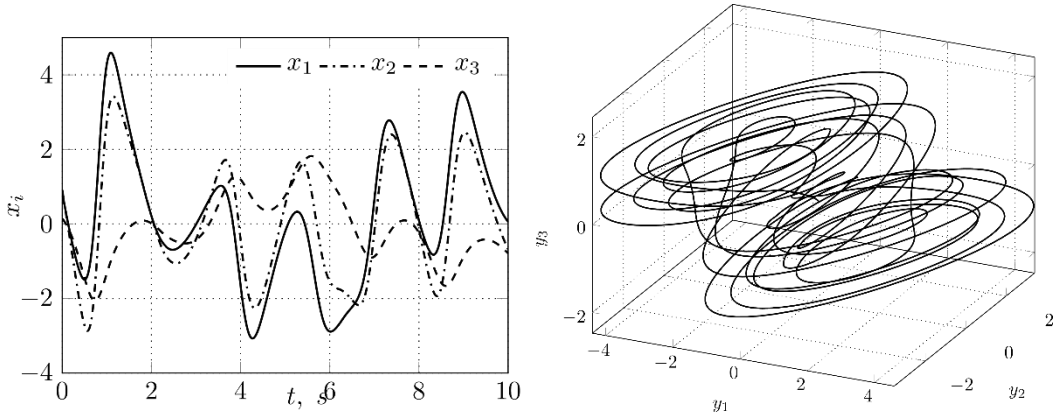

a) System outputs b) System 3D attractor

Figure 9: Simulation results of pendulum with observability equations (31) with variable factors.

Comparison of curves in Figure 7 – Figure 9 shows that the use of observability equations allows to increase the numbers of system outputs and transform its attractor from plane to space. Also, one can find that system dynamic becomes more complex when more factors have variable values. In Figure 10 we show simulation results for the case when one rewrite (32) with using of nonlinear functions:

$$\begin{gathered} x_1 = (y_1 - u_2)abs(u_1)\cos(\beta) + (u_1 - x_2)abs(y_1)\sin(\beta); \\ x_2 = (y_1 - u_2)abs(u_1)\cos(\beta + \alpha_1) + (u_1 - x_2)abs(y_1)\sin(\beta + \alpha_1); \\ x_3 = (y_1 - u_2)abs(u_1)\cos(\beta + \alpha_1 + \alpha_2) + (u_1 - x_2)abs(y_1)\sin(\beta + \alpha_1 + \alpha_2). \end{gathered} \quad (33)$$

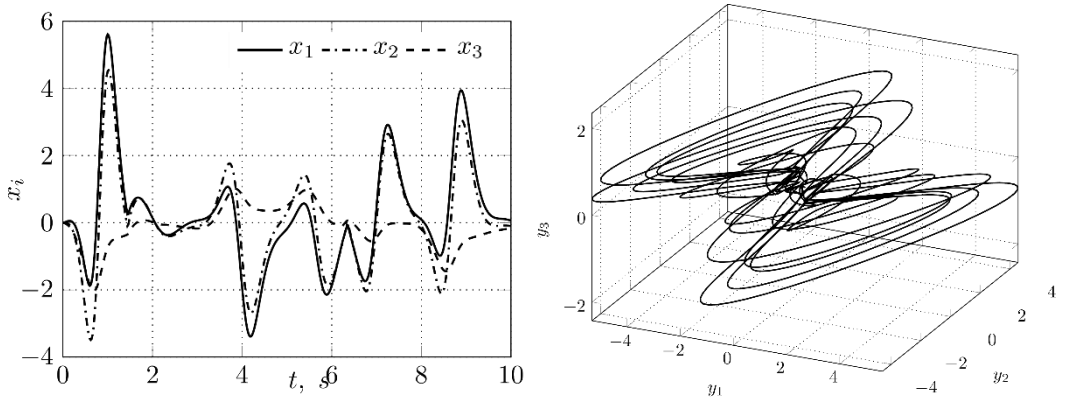

a) System outputs b) System 3D attractor

Figure 10: Simulation results of pendulum with observability equations (31) with variable factors.

Comparison of Figure 8 and Figure 10 shows that the use of nonlinear scale factor allows to form more complex system dynamic. As come can see from analysis of the above-given curves, the above-defined observability equations change systems attractors but they leave its two wings form.

In Figure 11 we illustrate the forming of system outputs with chaotic axes rotation angles by using following observability equations:

$$x_1 = (y_1 - u_2)abs(u_1)\cos(\beta) + (u_1 - x_2)abs(x_1)\sin(\beta);$$
$$x_2 = (y_1 - u_2)abs(u_1)\cos(\beta + \alpha_1) + (u_1 - x_2)abs(x_1)\sin(\beta + \alpha_1); \quad (34)$$
$$x_3 = (y_1 - u_2)abs(u_1)\cos(\beta + \alpha_1 + \alpha_2) + (u_1 - x_2)abs(x_1)\sin(\beta + \alpha_1 + \alpha_2).$$

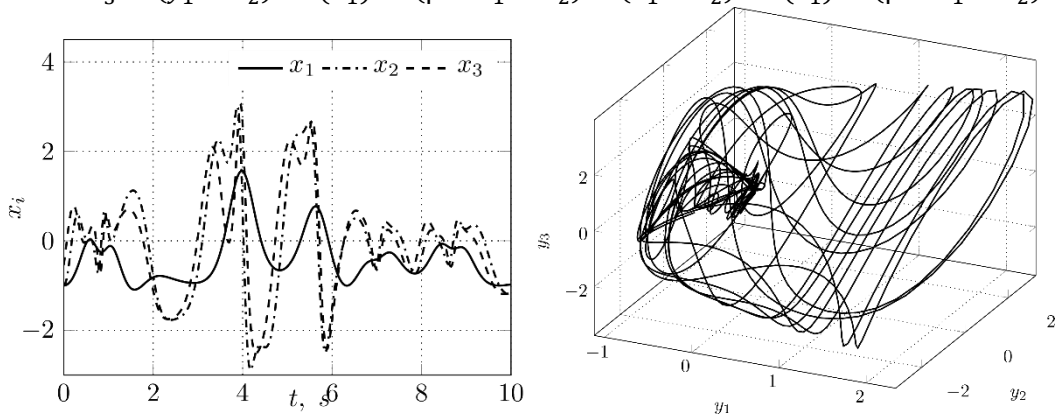

a) System outputs b) System 3D attractor

Figure 11: Simulation results of pendulum with observability equations (34).

As one can see the use of chaotic signals as argument of trigonometric functions in observability equations change the form of system attractor and does not allow to claim which system generates it.

All above-given in this subsection observability equations proves our approach and show ways to design discrete-time chaotic system as core closed-loop chaotic generator which produce some oscillations and some subsystem to post-process generated data.

3.3. Duffing pendulum model in M-dimensional non-orthogonal coordinates' plane

Let us show how to improve system features by performing one more post-processing of the generated data by transforming system from plane representation to space one. Such transformation can be performed if one takes into account (19) to define representative point position in some M-dimensional state space.

It is clear that components of (19) can be defined in a different ways, some of which is considered in previous subsection. To make system oscillations more complex we offer to rewrite (19) in terms of equations' (30) state variables as follows:

$$x_a = x_1 + y_1\cos(u_1);$$
$$y_a = x_2 + y_2\cos(u_2); \quad (35)$$
$$z_a = x_3 + y_1\sin(u_1) + y_2\sin(u_2).$$

Expression (35) are defined by using system state variables as well as its outputs in the plane models. It is clear that the above-given expression is one from possible variants to perform system transformation. We leave their studies for future researches.

Results of simulation (30) with observability equations (32) and (35) are shown in Figure 12.

As one can see applying observability equations to the initial generator equations allows to form output chaotic signals which are tremendously different from the known ones and have new attractor.

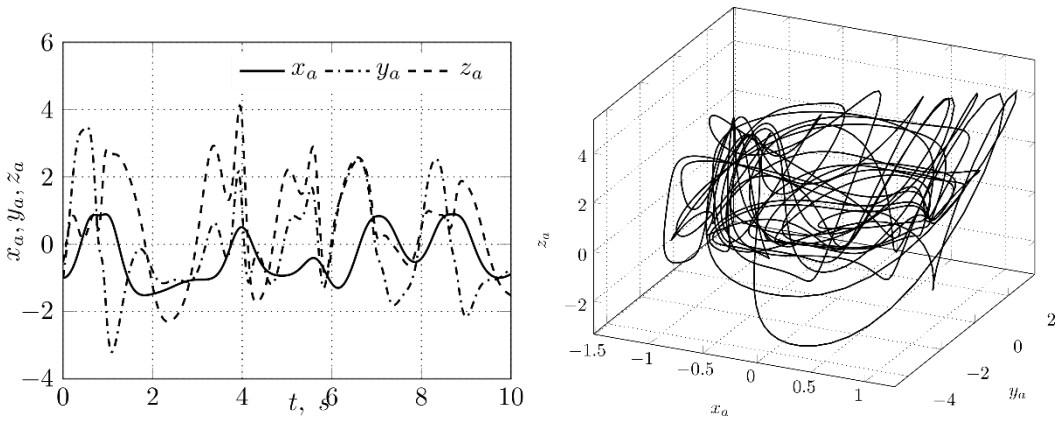

a) System outputs b) System 3D attractor

Figure 12: Simulation results of pendulum in 3D nonorthogonal coordinate system.

4. Conclusions

The considering of chaotic system as dynamical system in non-orthogonal coordinates gives us the possibility to produce novel chaotic oscillations by using well-known chaotic systems. This fact allows us to claim that novel chaotic system can be designed by changing one or both core system and system, which define transformations of coordinate system. In both cases system dynamic differs the core dynamic very much. The order of designed in such a way system equals to core system order Analysis of the obtained discrete-time models shows that chaotic system can be defined in class of discrete-time dynamical systems.

References

[1] C. Du, et al., An offset boostable hidden circuit and its digital information transmission, in: Proceedings of 13th Annual Ubiquitous Computing, Electronics & Mobile Communication Conference (UEMCON), IEEE, New York, USA, 2022, pp. 187–194. doi: 10.1109/UEMCON54665.2022.9965685.

[2] H. A. Naser, et al., Utilizing a high-sensitive and secure communication system for data transmission, in: Proceedings of Second International Conference on Advanced Computer Applications (ACA), Misan, Iraq, 2023, pp. 1–5. doi: 10.1109/ACA57612.2023.10346881.

[3] W. Wu, et al., Novel secure data transmission methods for IoT based on STP-CS with multilevel critical information concealment function, IEEE Internet of Things Journal 10(5) (2023) 4557–4578. doi: 10.1109/JIOT.2022.3218681.

[4] E. A. Umoh, et al., Chaos theory applied to cascading disaster dynamics, modelling and control, in: Proceedings of Nigeria 4th International Conference on Disruptive Technologies for Sustainable Development (NIGERCON), IEEE, Lagos, Nigeria, 2022, pp. 1–4. doi: 10.1109/NIGERCON54645.2022.9803084.

[5] A. Ascoli, et al., Edge of chaos theory resolves Smale paradox, IEEE Transactions on Circuits and Systems I: Regular Papers 69(3) (2022) 1252–1265. doi: 10.1109/TCSI.2021.3133627.

[6] J. Xie, et al., A network covert timing channel detection method based on chaos theory and threshold secret sharing, in: Proceedings of 4th Information Technology, Networking, Electronic and Automation Control Conference (ITNEC), IEEE, Chongqing, China, 2020, pp. 2380–2384. doi: 10.1109/ITNEC48623.2020.9085024.

[7] S. Warjri, et al., Radar communication via asymmetric and wideband chaotic signal, in: Proceedings of 5th International Conference on Energy, Power and Environment: Towards Flexible Green Energy Technologies (ICEPE), IEEE, Shillong, India, 2023, pp. 1–6. doi: 10.1109/ICEPE57949.2023.10201586.

[8] R. A. da Costa, M. Eisencraft, Chaotic signals representation and spectral characterization using linear discrete-time filters, in: Proceedings of 28th European Signal Processing Conference (EUSIPCO), IEEE, Amsterdam, Netherlands, 2021, pp. 2235–2238. doi: 10.23919/Eusipco47968.2020.9287475.
[9] H. Bian, et al., Parameter inversion of high-dimensional chaotic systems using neural ordinary differential equations, in: Proceedings of 13th Data Driven Control and Learning Systems Conference (DDCLS), IEEE, Kaifeng, China, 2024, pp. 400–405. doi: 10.1109/DDCLS61622.2024.10606602.
[10] M. Beisenbi, et al., Control of deterministic chaotic modes in power systems, in: Proceedings of International Conference on Smart Information Systems and Technologies (SIST), IEEE, Astana, Kazakhstan, 2023, pp. 516–521. doi: 10.1109/SIST58284.2023.10223493.
[11] P. Liu, et al., Dynamic analysis of novel memristor chaotic systems with influence factors, in: Proceedings of International Conference on Electrical, Automation and Computer Engineering (ICEACE), IEEE, Changchun, China, 2023, pp. 118-122, doi: 10.1109/ICEACE60673.2023.10441899.
[12] V. Rusyn, et al., Computer modelling, analysis of the main information properties of memristor and its application in secure communication system, in: Proceedings of The Seventh International Workshop on Computer Modeling and Intelligent Systems (CMIS-2024), Zaporizhzhia, Ukraine, 2024, pp. 216–225.
[13] V. Rusyn, et al., Computer modelling of the three-dimensional new chaotic system using Labview, Collection of Scientific Papers «ΛΌГОΣ», Cambridge, UK, 2024, pp. 307–310. doi: 10.36074/logos-29.03.2024.065.
[14] R. Voliansky, et al., Multi-channel chaotic system, in: Proceedings of 10th International Conference on Advanced Computer Information Technologies (ACIT), IEEE, Deggendorf, Germany, 2020, pp. 196–199. doi: 10.1109/ACIT49673.2020.9209000.
[15] R. Voliansky, et al., Design of the generalized infinite-dimensional chaotic system, in: Proceedings of 5th International Conference on Advanced Information and Communication Technologies (AICT), IEEE, Lviv, Ukraine, 2023, pp. 193–197. doi: 10.1109/AICT61584.2023.10452667
[16] X.-Y. Hu, et al., A chaotic pseudo orthogonal covert communication system, in: Proceedings of 6th International Conference on Communication and Information Systems (ICCIS), IEEE, Chongqing, China, 2022, pp. 61–65. doi: 10.1109/ICCIS56375.2022.9998136.
[17] C. E. C. Souza, et al., A symbolic dynamics approach to trellis-coded chaotic modulation, IEEE Transactions on Circuits and Systems II: Express Briefs 67(10) (2019) 2189–2193. doi: 10.1109/TCSII.2019.2953158.
[18] H. Wang, et al., Secure transmission design for dual-polarized satellite system via DL-MPWFRFT and improved chaotic phase modulation, in: Proceedings of International Conference on Wireless Communications and Signal Processing (WCSP), Nanjing, China, 2020, pp. 424–429. doi: 10.1109/WCSP49889.2020.929978.
[19] R. Munirathinam, et al., Chaotic non-coherent pulse position modulation based ultra- wideband communication system, in: Proceedings of Microwave Theory and Techniques in Wireless Communications (MTTW), IEEE, Riga, Latvia, 2021, pp. 1–6. doi: 10.1109/MTTW53539.2021.9607075.
[20] R. Voliansky, A. Sadovoi, Chua's circuits interval synchronization, in: Proceedings of 4th International Scientific-Practical Conference Problems of Infocommunications. Science and Technology (PIC S&T), IEEE, Kharkov, Ukraine, 2017, pp. 439–443. doi: 10.1109/INFOCOMMST.2017.8246434.
[21] R. Voliansky, A. Sadovoy, Chua's circuits synchronization as inverse dynamic's problem solution, in: Proceedings of Third International Scientific-Practical Conference Problems of Infocommunications Science and Technology (PIC S&T), IEEE, Kharkiv, Ukraine, 2016, pp. 171–172. doi: 10.1109/INFOCOMMST.2016.7905371.

[22] Y. Xing, et al., Research on improved generalized chaotic synchronization method based on 6-D discrete chaotic systems, in: Proceedings of 2nd International Joint Conference on Information and Communication Engineering (JCICE), IEEE, Chengdu, China, 2023, pp. 105–110. doi: 10.1109/JCICE59059.2023.00030.
[23] L. Mingye, et al., Chaotic feature masking against attacks on emitter identification, in: Proceedings of 22nd International Conference on Optical Communications and Networks (ICOCN), IEEE, Harbin, China, 2024, pp. 1–3. doi: 10.1109/ICOCN63276.2024.10648408.
[24] M. Li, et al., Chaotic radio frequency fingerprint masking against identity attacks, IEEE Wireless Communications Letters 13(9) (2024) 2616–2619. doi: 10.1109/LWC.2024.3434453.
[25] S. Guo, et al., Blind source separation algorithm for chaotic masking multipath signals based on spectral peak search counter permutation, IEEE Access 8 (2022) 86617–86629. doi: 10.1109/ACCESS.2020.2993305.
[26] V. Oliinyk, V. Lukin, Time delay estimation for noise-like signals embedded in non-Gaussian noise using pre-filtering in channels, in: Proceedings of IEEE 15th International Conference on Advanced Trends in Radioelectronics, Telecommunications and Computer Engineering (TCSET), IEEE, Lviv-Slavske, Ukraine, 2020, pp. 638–643. doi: 10.1109/TCSET49122.2020.235510.
[27] Z. Kolodiy, A. Kolodiy, Detection of informational signal among noisy signals, in: Proceedings of International Conference on Noise and Fluctuations (ICNF), IEEE, Grenoble, France, 2023, pp. 1–4. doi: 10.1109/ICNF57520.2023.10472749.
[28] A. Z. R. Langi, et al., An overview of fractal processing of noise-like auditory signals, in: Proceedings of International Conference on ICT for Smart Society (ICISS), IEEE, Bandung, Indonesia, 2021, pp. 1–4. doi: 10.1109/ICISS53185.2021.9533247.
[29] T. Fan, et al., A new APSK-based M-Ary differential chaos shift keying modulation system, IEEE Communications Letters 24(12) (2020) 2701–2704. doi: 10.1109/LCOMM.2020.3019105.
[30] J. Zheng, et al., An orthogonal time frequency space modulation based differential chaos shift keying transceiver for reliable communications, in: Proceedings of 97th Vehicular Technology Conference (VTC2023-Spring), IEEE, Florence, Italy, 2023, pp. 1–5. doi: 10.1109/VTC2023-Spring57618.2023.10201217.
[31] H. Wang, et al., Secure transmission design for dual-polarized satellite system via DL-MPWFRFT and improved chaotic phase modulation, in: Proceedings of International Conference on Wireless Communications and Signal Processing (WCSP), IEEE, Nanjing, China, 2020, pp. 424–429. doi: 10.1109/WCSP49889.2020.9299787.
[32] R. Voliansky, et al., Interval modeling and simulation of duffing pendulum, in: Proceedings of 4th KhPI Week on Advanced Technology (KhPIWeek), IEEE, Kharkiv, Ukraine, 2023, pp. 1–6. doi: 10.1109/KhPIWeek61412.2023.10312997.
[33] O. Solomentsev, et al., Efficiency analysis of current repair procedures for aviation radio equipment, in: I. Ostroumov, M. Zaliskyi (Eds.), Proceedings of the 2nd International Workshop on Advances in Civil Aviation Systems Development. ACASD 2024, volume 992 of Lecture Notes in Networks and Systems, Springer, Cham, 2024, pp. 281–295. doi: 10.1007/978-3-031-60196-5_21.
[34] M. Zaliskyi, et al., Methodology for substantiating the infrastructure of aviation radio equipment repair centers, CEUR Workshop Proceedings 3732 (2024) 136–148. URL: https://ceur-ws.org/Vol-3732/paper11.pdf.